DATE DUE	DATE DUE	DATE DUE

EXPERIMENTAL STUDY OF MIXING OF DIRECTLY INJECTED FUEL WITH AIR IN AN OPTICALLY ACCESSIBLE ENGINE USING LASER INDUCED FLUORESCENCE

By

Jon Clayton Darrow

A THESIS

Submitted to
Michigan State University
In partial fulfillment of the requirements
For the degree of

MASTER OF SCIENCE

Department of Mechanical Engineering

1998

ABSTRACT

Experimental Study of Mixing of Directly Injected Fuel with Air in an Optically Accessible Engine Using Laser Induced Fluorescence

By

Jon Clayton Darrow

Most of today's automobiles burn petroleum fuels. A limited supply of these fuels requires that we pursue various avenues to conserve the existing quantities. One way that will help conserve these supplies is by increasing the efficiency of internal combustion engines. For our national economy, it is important to reduce pollution and the gases that influence global warming. One way to obtain these goals is by improving the efficiency and by better understanding the mixing of the fuel and the air in an internal combustion engine. To help us understand this process, a suitable chemical tracer was added to the liquid fuel. Using a laser to excite this chemical resulted in fluorescence light emission that was quantified through an extensive in-cylinder calibration. This proved to be a good technique since this chemical showed little effect of oxygen quenching, which enabled a realistic engine experiment. In order to perform this type of study in an engine, one needs optical access to the combustion chamber. This was accomplished by constructing a single-cylinder, optically accessible engine. The construction of such a rig and performing a quantitative analysis of the fuel and air mixing are the foci of this work.

Acknowledgments

I would like to thank Dr. Harold Schock for providing me with the opportunity to do research at the MSU Engine Research Lab. I would like to thank Dr. JongUk Kim for his help in the data acquisition and answers for the many questions raised on optics and photochemistry. I would also like to thank Dr. Giles Brereton and Keunchul Lee for listening to my questions and providing insight to experimental testing. Thanks goes to Tom Stuecken for his suggestions and help in building the experimental setup and the taking of the high-speed films. I would also like to thank Mark Novak and Matt Foster for their help with the post processing of the data and computer-related matters. Dr. Gary Vanee, Richard Ledebuhr, and Richard Wolthuis provided their suggestions for the experimental setup and gave me access to the machine shop at Agriculture Engineering. My lab friends Larry Dalimonte, Mikhail Ejakov, Hans Hascher, and Mahmood Rahi for many good times.

My greatest thanks goes to my parents June and Bob Heilman for supporting me through the additional time that was needed for an advanced degree. Kelly Aichler was also understanding during the long hours and weekends that were dedicated to studying and doing research.

I thank Chrysler Corporation, General Motors, National Science Foundation, and MSU Manufacturing Research Consortium for making this research project possible.

TABLE OF CONTENTS

LIST OF TABLES

LIST OF FIGURES

CHAPTER 1

INTRODUCTION

1.1 Literature Review

Over the years, different measurement techniques, such as Laser Doppler Velocimetry (LDV), high speed photography and Laser Induced Fluorescence (LIF), have been used in an effort to understand the mixing processes of fuel and air in an internal-combustion engine. Of these different techniques, Laser Induced Fluorescence (LIF) has become a popular method of visually quantifying the mixing processes. Since pure isooctane, which is the base ingredient to commercial gasoline, does not fluoresce, there is a need for additional additives, that do fluoresce. In order for these chemical tracers to give reasonable results they need to be soluble in isooctane and have similar physical characteristics as isooctane. There are a number of tracers that fit these criteria, each with its own advantages and disadvantages.

Laser Induced Exciplex Fluorescence (LIEF), which uses naphthalene and tetramethyl-p-phenylene (TMPD) as the tracers, was developed by Melton for visualization of evaporating diesel fuel sprays. These chemicals form excited state complexes (exciplexes) that have the ability to provide spectrally separate liquid and vapor phases. The vaporization characteristics of the tracers and the diesel fuel are similar

so the tracking of the liquid and vapor is reasonably accurate. [1, 2] More recently, technique has been applied to ignition engines using N, N-dimethylaniline (DMA) and trimethylaphthalene (1,4,6-TMN) [3]. These chemicals form an excited state complex, but they are not co-evaporative with gasoline. These chemicals have boiling points that are approximately twice that of gasoline at a given pressure and tend to underestimate the mass in the vapor phase. The boiling point of DMA is 193° C and isooctane is 98-99° C. These chemical systems exhibit oxygen quenching, which proves to be a serious impediment in combustion engine experiments. This oxygen-quenching problem also eliminates this technique from consideration for firing engine experiments. [4, 5] Other LIF techniques use isooctane with commercial gasoline added for the fluorescing tracer. Due to the unknown chemical composition of the gasoline, quantitative calibration is not applicable [6, 7]. Chemical tracers such as 3-pentanone (ethelketone) have been shown to be favorable as a laser induced tracer for use with isooctane. The many advantages it has are that it is soluble in isooctane, has a similar vapor pressure curve, and has a very similar boiling point to isooctane. Its biggest advantage is its ability to fluoresce in an oxygen environment. A disadvantage, like other single tracer LIF techniques, is that it does not spectrally distinguish the liquid and vapor phases. [8- 11]

Using these chemical systems to study the flow inside an internal combustion engine requires optical access into the engine cylinder. A configuration, that has a quartz cylinder and Bowditch [12] style quartz crowned piston is required. Many different designs have been built in the past by other researchers for similar studies. The main requirement for such an engine is viewing access of the combustion chamber close to top dead center. Some research engines have been built with small quartz widows in the side

of the cylinder for access. [13, 14] Another approach is to use a complete quartz cylinder with nonabrasive plastic piston rings. [4, 15] This modification provides the most unobstructed optical access but gives up some structural integrity if combustion experiments are to be used. Since this study is for precombustion fuel-air preparation, it could be conducted in a motored condition. This configuration can be used for other visualization and velocity measuring techniques. Therefore, the research engine was modified for the most optical access.

1.2 Introduction to Laser Induced Fluorescence

Molecules such as some ketones have the ability to absorb certain wavelengths of light and form excited states of the molecules. When 3-Pentanone absorbs ultraviolet light it is excited to the first singlet State (S*). Once in this state it has four options to return to the ground state. Details of the absorption and emission spectra are given later. Fluorescent emission occurs when radiation is emitted during the transition from the excited state to the ground state. The excited state may also return to ground state by internal conversion whereas the transition to ground state is radiationless. Intersystem crossing refers to a radiationless transition between states of different multiplicity. This can be seen in Figure 1. [16]

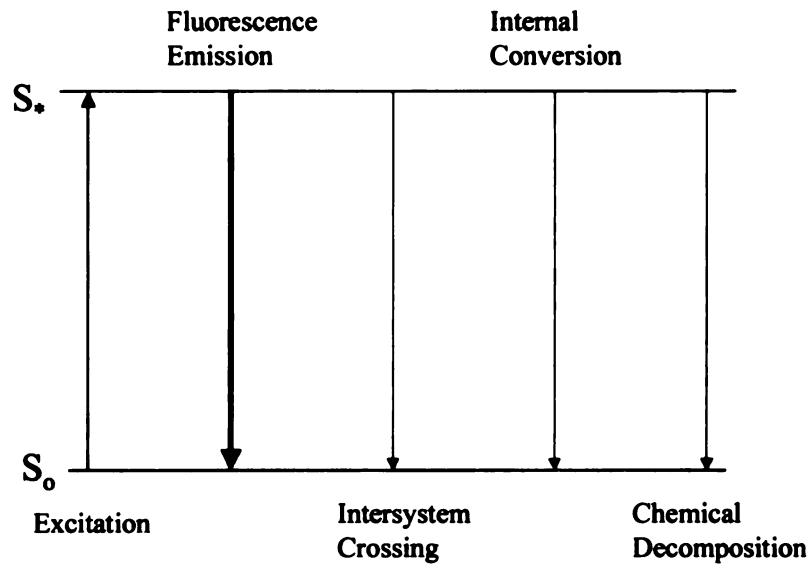

Figure 1. Deactivation Processes of 3-Pentanone [16]

The general photochemical properties of 3-pentanone are the main reason that this chemical was used in the current study. It has an absorption spectrum in the range of 220 – 320 nm with a peak at 280 nm, which is shown in Figure 2. This enables one to use an Eximer laser at 308 nm for an excitation light source. This excitation wavelength is on the trailing edge of the absorption spectra but was deemed to be acceptable. The emission spectrum is in the range of 300 to 600 nm, with a maximum of about 450nm as shown by Figure 3. The one disadvantage of using this chemical is that the fluorescent emission process makes up less than one percent of the total deactivation [17]. The major advantage of using 3-pentanone for a fluorescing tracer for gasoline is that is has similar vaporization characteristics as isooctane, as shown in Figure 4. The boiling points are also similar to isooctane's boiling point 98-99° C at ambient pressure and 3-Pentanone's boiling point of 102° C.

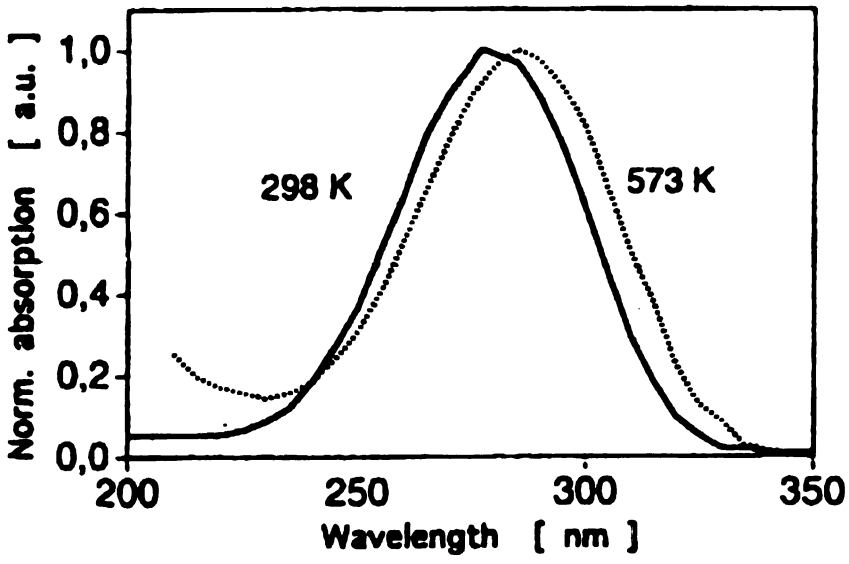

Figure 2. Absorption Spectrum of 3-Pentanone at Different Temperatures and Atmospheric Pressure [18]

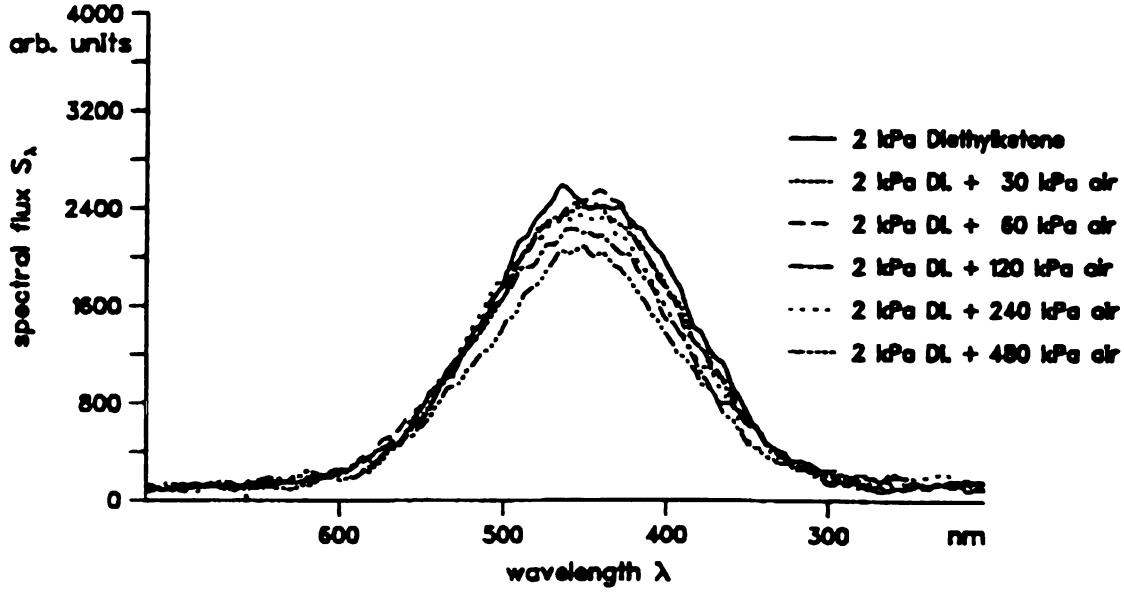

Figure 3. Fluorescence Spectra of 3- Pentanone (Diethylketone) [9]

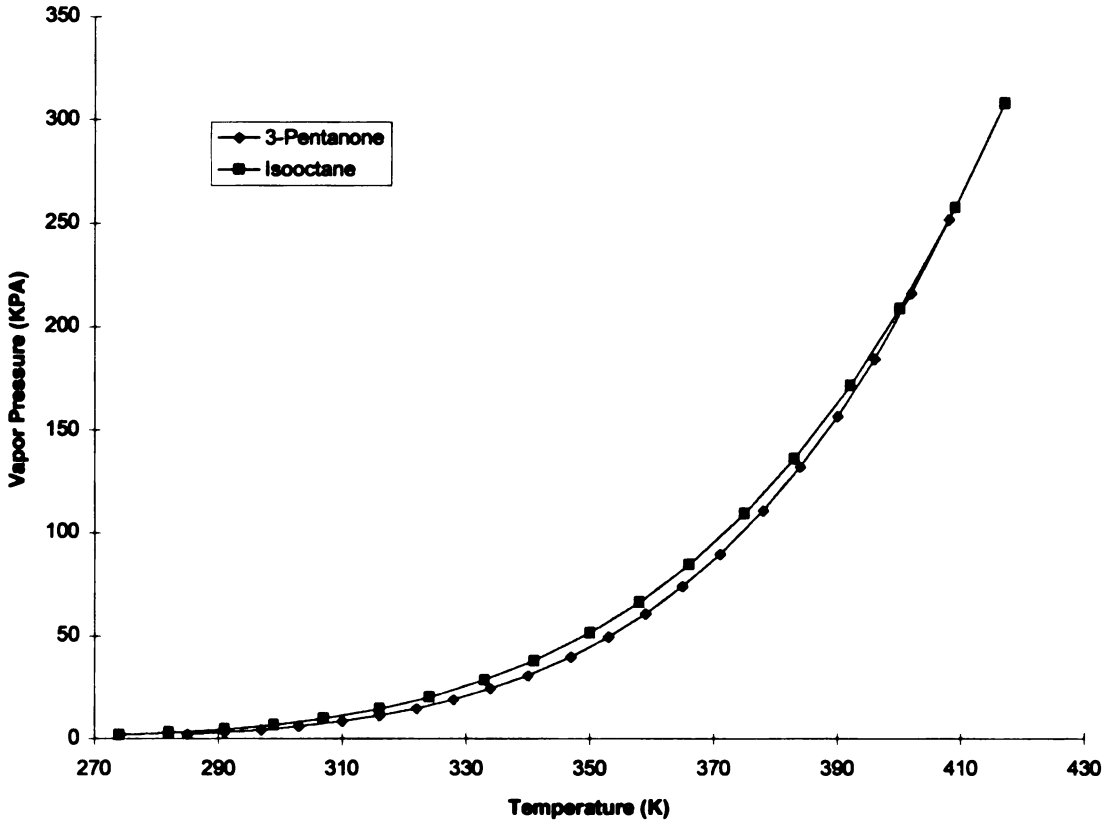

Figure 4. Temperature vs. Vapor Pressure for 3-Pentanone and Isooctane [19]

1.3 Objectives of the Study

The objectives of this study are given below. They are:

- Construct an optically accessible research engine for use with laser induced fluorescence methods and other in-cylinder measuring techniques.
- Design and build a premixing system that provides a known equivalence ratio to the motored research engine with the range of 0.2 to 2.0.
- Develop an in-cylinder calibration procedure using a 3-Pentanone in isooctane mixture for quantifying local air/fuel ratios.
- Determine the effectiveness of the LIF technique by evaluating local air/fuel ratios in a Chrysler prototype direct injected cylinder head.

The results which describe the progress made on each of these objectives are described in the following sections.

CHAPTER 2

OPTICAL ENGINE AND PREMIXING INTAKE SYSTEM

2.1 Optical Engine

An AVL single cylinder research engine was modified with a quartz cylinder and an elongated piston, which contained a quartz-piston crown. A 2.4 liter 4 cylinder direct injected Chrysler cylinder head was mounted on top of the reciprocating engine base. Only one combustion chamber was used in the study. A separate intake system was designed to deliver a preheated mixture of fuel and air to the engine for the calibration. The requirements for the design of an optical engine for this type of testing are to obtain as much optical access from the side and through the piston top. This optically accessible combustion chamber permits flow studies in planes parallel and perpendicular to the piston surface. The reason for such broad requirements is that the engine was used for multiple in-cylinder experiments. In addition to the laser induced fluorescence experiments, which were conducted in the engine for this project, flow visualizations of single direct injection events were taken using high-speed photography. Exciplex laser induced fluorescence studies and initial tests of a new velocity measuring technique called Molecular Tagging Velocimetry (MTV) were also examined using this engine assembly.

Specifications for the optically accessible engine are given in Table 1. Another major requirement when using a research engine of this type for LIF and flow visualization experiments is the need to frequently clean the optical surfaces. To reduce the time for cleaning, the test rig was designed for ease of assembly and disassembly. A photo of the completed engine assemble is in Figure 5 and a photo of the complete LIF setup is in Figure 6. The details of the major engine components are described in the following subsections.

Table 1. Optical Engine Specifications

Number of Cylinders	1
Bore	87.5 mm (3.444 in)
Stroke	100mm (3.937 in)
Rod Length	178 mm (7.01 in)
Compression Ratio	9.4 to 1
Number of Valves	Inlet: 2 Exhaust: 2
Intake Valve Opening	51 ATDCI
Intake Valve Closing	171 ATDCI
Exhaust Valve Opening	562 ATDCI
Exhaust Valve Closing	668 ATDCI

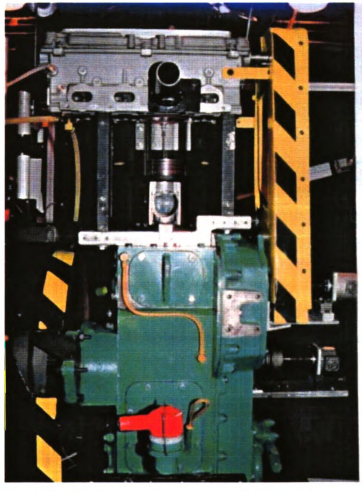

Figure 5. Optical Engine Assembly

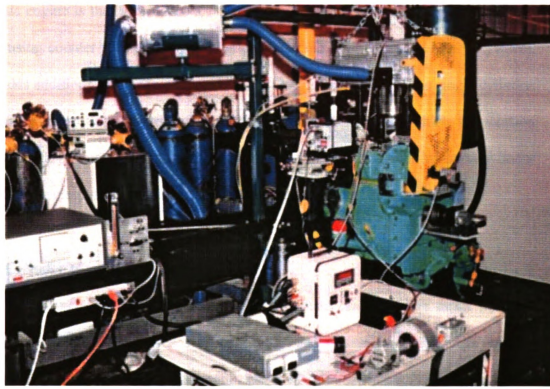

Figure 6. Laser Induced Fluorescence Experimental Test Assembly

2.1.1 Crankcase

The reciprocating mass is an AVL 530 crankcase and cylinder. The advantage of using this engine is that it provides a first-order balance for rotational and reciprocating masses using counter-rotating balance shafts. The crank is fitted with a heavy flywheel, which adds additional inertia in order to maintain a constant speed for the single cylinder. The crankcase has been refitted with a 100-mm stroke crankshaft, which was custom built by Moldex Cranks [20] to match the stroke of the Chysler direct injection cylinder head. No balancing of this assembly was needed for the current experiments.

2.1.2 Cylinder Head

The cylinder head is a 2.4-liter, double overhead cam, Chrysler direct injection prototype. It contains four valves, two spark plugs, and a centrally located high-pressure prototype injector. A diagram of the combustion chamber is shown in Figure 7. In this experiment only the number 2 combustion chamber is used. The lifters of all other cylinders have been removed to actuate only the required valves. The cylinder head is mounted above the engine on two supports, and a quartz cylinder and steel spacer is placed between, as in Figure 8.

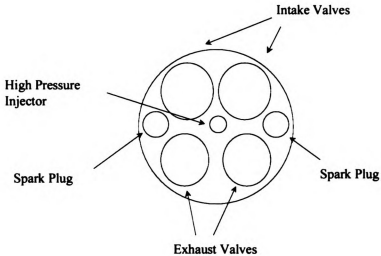

Figure 7. Direct Injection Combustion Chamber

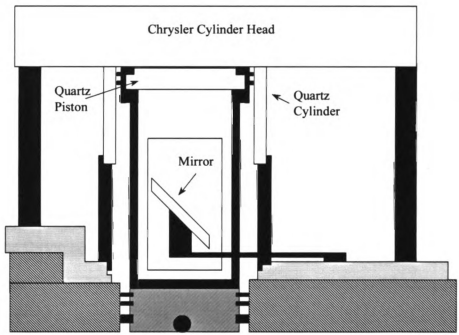

Figure 8. Schematic of Optical Engine

The cylinder head is mounted to the supports by four bolts. These bolts enter from the bottom through the supports into threaded inserts that were installed in the head. This allows easy removal of the head for cleaning without removing valve covers or resealing oil drain passages. The alignment of the cylinder head to the supports is critical when using this type of quartz cylinder design, so a series of four aligning pins were used. An additional ringed support was added to the cylinder head to provide a means of locating the quartz cylinder. The cylinder head lubrication is separate from the crankcase because the cylinder head does not sit at the same angle as in the original engine, which creates oil-draining problems. An oil pump draws oil from a reservoir and supplies it to an inlet passage in the head at a pressure of 20 psi. Oil draining of the head is accomplished by applying a slight vacuum to the return lines installed in the return passages of the cylinder head.

2.1.3 Quartz Cylinder and Piston

The quartz cylinder is made of GE 124 fused quartz, which has a transmissivisty of 92% in the range of UV light that is being used. The cylinder was chosen to be 10mm (0.394 in) thick, which provided enough strength without significant loss of laser power. This quartz cylinder was sealed to the cylinder head by using two O-rings in a Rulon® spacer. One O-ring is sealed against the head and the other is sealed against the top edge of the quartz. The quartz piston top insert is also made of GE 124 fused quartz and is 17.78mm (0.700 inches) thick. The quartz-piston crown provides optical access over about 62% of the piston area. This provides good optical access to the combustion

chamber when the piston is close to TDC. A view through the piston into the cylinder with the piston at TDC is shown in Figure 9.

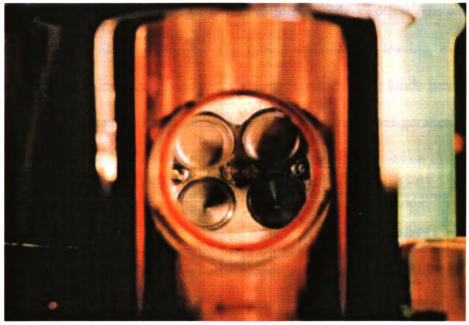

Figure 9. View Through Quartz Piston with Piston at Top Dead Center

2.1.4 Piston Extension

The piston extension, which was machined from billet 70705 T651 aluminum for a high strength to weight ratio, is a hollow tube with a slot cut in one side. This provided access for a stationary mirror, which allowed viewing into the cylinder. This extension is bolted directly to the top of the AVL piston with six 5/16-inch counter sunken screws. The piston top is a screw on top design, which retains the quartz piston top insert. The piston top has internal threads and the extension has matching external threads. This type of design also allows different piston configurations to be used. Torlon® piston rings provided good sealing without damaging the quartz cylinder or leaving excessive deposits on the cylinder. Since the piston had a quartz insert, the ring lands were much shorter than those in a conventional piston. Several ring-pack configurations were examined, and it was found that a slight taper of approximately 2 degrees on the face of the ring with the taper positioned such that the outer contact edge was on top provided the best sealing. The grade of Torlon® used was 4301. This material is a thermoplastic, which exhibits exceptional physical and chemical properties. It has resistance to high temperature (246° C), never needs lubrication, and has a low coefficient of friction. These properties make it an ideal nonabrasive piston ring material for the quartz cylinder.

2.1.6 High Pressure Fuel Injection System

The control of the fuel to the high-pressure injector for the in-cylinder direct injection was accomplished by a custom-designed electronic system. This electronic control box uses input from a 360-degree, Dynapar, shaft-angle encoder. This encoder was attached to the cam take-off of the AVL with a flex coupling. This cam take-off is

geared internally to a two-to-one ratio, which allows the encoder to spin once for every two revolutions of the crankshaft. The control box provides a 5-volt TTL trigger signal-out, which is required for the synchronization of the laser and the ICCD camera. This trigger signal has sufficient adjustable delay to allow the laser pulse and camera to capture an image at any point in the cycle. The fuel injection, pulse-out signal, which is also adjustable anywhere in the cycle, is sent to a special control device, which operates the high-pressure injector. This special control device which was provided by Chrysler, contained the electronic control module from an automobile with additional circuitry. The control box also contains a digital readout tachometer for accurate rpm readings. The fuel system that delivers fuel to the high-pressure injector is made up of a fuel reservoir from which a low-pressure (60-psi) 12-volt pump draws fuel. This low-pressure pump primes the high-pressure pump, which is driven by a ½ horsepower electric motor. A schematic of the system is shown in Figure 10.

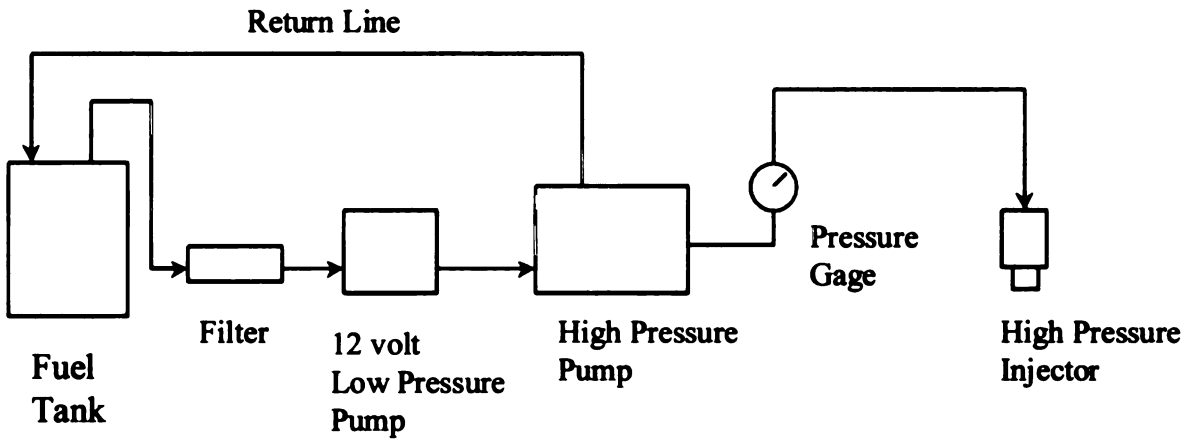

Figure 10. Schematic of High-Pressure Fuel System

2.2 Intake System

A special intake system for the 3-pentanone calibration was constructed to supply a homogeneous mixture of fuel and nitrogen or air to the engine in order to obtain a given fluorescence intensity for each equivalence ratio at different crank angle positions in the engine. Equivalence ratio ϕ, is defined as the fuel air ratio f/a, to the stoichiometric fuel air ratio $(f/a)_s$, as in equation (1).

$$\phi = \frac{f/a}{(f/a)_s} \tag{1}$$

The intake system for the calibration consists of a nitrogen balance system, laminar flow element (LFE), intake heater assembly, fuel injection zone, mixing zone, and an intake plenum. The intake system for the in-cylinder, direct injection engine measurements is similar to the calibration setup except that the orifice injection system is not used. A schematic of the premixing intake system is shown in Figure 11. The design objectives of this system were to provide an atomized and vaporized mixture of either air or nitrogen and fuel to a motored engine and to accurately monitor these quantities. The system is sized for a theoretical single cylinder of approximately 0.6 liters at a maximum speed of 1500 rpm and wide-open throttle with a range of equivalence ratios from 0.2 to 2.0.

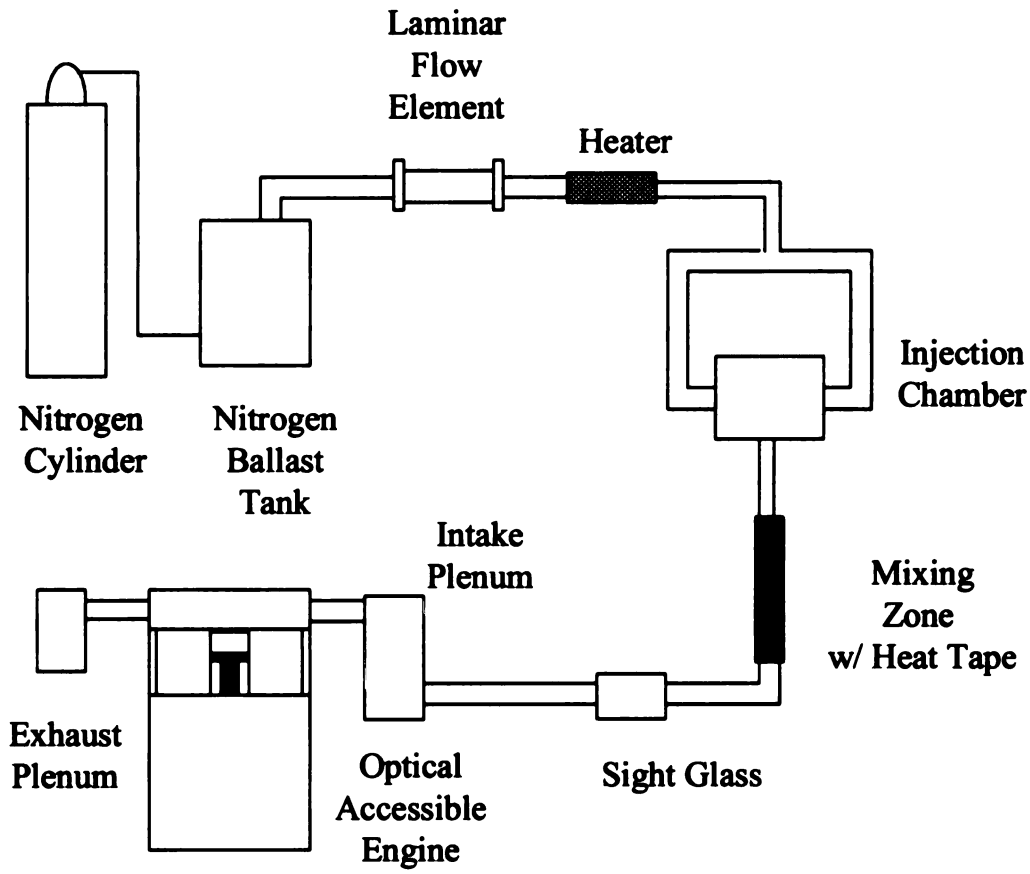

Figure 11. Schematic of Premixing Intake System

The nitrogen-balance system, working as an accumulator, consists of a 55-gallon container with a plastic diaphragm attached to act as a visual flow-balancing device. Nitrogen is delivered from compressed nitrogen tanks to the bottom of the container. The outlet is via the top through a two-inch diameter flexible hose. The nitrogen gas flow rate is monitored by the laminar flow element installed at the outlet of the tank.

The Laminar Flow Element (LFE) is a model 50mh10-1 ¼ from Meriam Instrument, rated at 17.0 Standard Cubic Feet per Minute (SCFM) and 8 inches of water differential. This unit was mounted between an upstream tube length of 15 inches and a downstream tube length of 7 inches to ensure laminar flow. These dimensions correspond to a 10 diameter inlet tube length and 5 diameter outlet length, which is recommend by Meriam to ensure accurate readings. The differential pressure ports were connected to a Meriam inclined-tube manometer, which displayed the flow rate in Cubic Feet per Minute (CFM). The inclined-tube manometer used was model 40HE35 with a maximum capacity of 8 inches of water differential, which allows for 17 SCFM to flow through the element. To obtain accurate reading the flow rate in CFM was corrected for measured inlet temperature, ambient pressure and adjusted for the pure nitrogen.

The nitrogen then passed through a heater assembly. The heater element consists of a 300-500 watt, heat-gun, replacement element. This heater assembly is automatically controlled by an API Instruments Co. closed-loop, thermocouple, control unit. The temperature was maintained at 100° C. Heated nitrogen is drawn into an injection chamber where the atomized fuel is introduced. This injection chamber is made up of an aluminum block with the nitrogen entering at 90 degrees to the fuel inlet.

The fuel injection calibration system consists of pressurized fuel passing though precision orifices. The fuel was pressured by nitrogen in a pressure vessel, which delivers the fuel at a given pressure without pulsation. The fuel then passes through two sintered, metal filters: first a 7-micron and then a 2-micron. Next, the fuel flowed through a shut-off valve and pressure gage and on to the fuel metering orifices. These orifices have a cross section as in Figure 12. The orifices were polycrystalline diamond wire extrusion

dies produced by Hoosier Wire and Die. The die sizes that provided the necessary flow rate were 0.003, 0.004, 0.005, and 0.006 inches in diameter. Once the isooctane, 3-Pentanone mixture was injected into the nitrogen stream, the mixture passed though a mixing chamber consisting of spiral wound wire screen of varying mesh size. This chamber was heated using heating tape and controlled with a Variac to maintain an elevated temperature to ensure liquid evaporation. A sight glass was installed in line to ensure that the mixture was in vapor form and that no liquid fuel was on the walls.

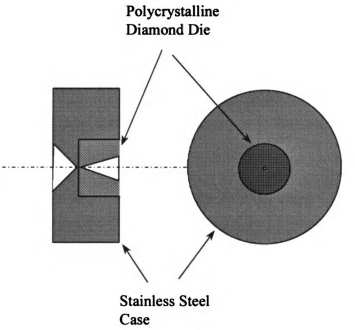

Figure 12. Cross Section View of Fuel Metering Orifices

This vaporized fuel and nitrogen mixture then passed though a 1-meter, insulated tube to ensure fully developed flow and complete mixing. The mixture entered the intake plenum, consisting of a 15-gallon tank with a pressure and vacuum relief. This size was chosen according to the SAE J1088 small engine test procedure, which states that at least 100 times the cylinder volume is needed to obtain accurate average flow rates when using the laminar flow element. The mixture then passes though a straight section of manifold to the intake side of the cylinder head. This section of manifold is where the temperature and sample probes were located. After the mixture has been through the cylinder, it entered an exhaust plenum and then a fan removed the mixture from the building.

To verify if this system would handle the capacity of fuel that was needed, the maximum amount of fuel that would remain in vapor form at a given temperature was calculated, using Dalton's Law (2) under assumption of an ideal gas [21]. It is assumed that when fuel is injected into an air stream it will start to evaporate and will continue until it has completely evaporated. At 600 rpm and an equivalence ratio of 2.0 the fuel supply rate is approximately 0.42 g/sec. To assure that this amount of fuel remains in vapor for the temperature needs to remain at 20° C or more. At 1500 rpm and an equivalence ratio of 2.0 the fuel supply rate is 1.22 g/sec. The saturation vapor temperature for this amount of fuel is also less than 20° C. It was concluded that as long as the temperature in the intake runner of the motor engine remained above 25° C, all of the injected fuel that was vaporized would remain in vapor. This result is shown in Figure 13.

$$f_v = \frac{m_{fv} p_f}{29(p - p_f)} \qquad (2)$$

Where,

f_v = Mass ratio of fuel to air
m_{fv} = Average molecular weight of the fuel vapor
p_f = Partial pressure of the fuel vapor
p = Total pressure of the mixture

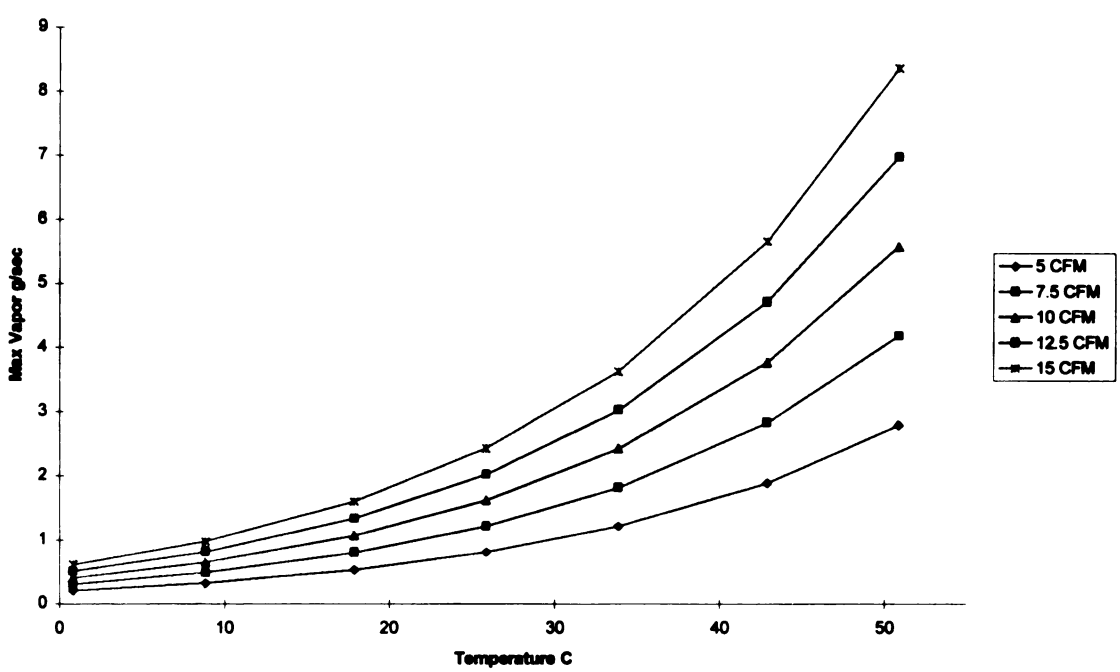

Figure 13. Temperature vs. Maximum Vapor of Isooctane in Air

2.3 Hydrocarbon Analyzer

A flame ionization detector (FID), Beckman model 400 Hydrocarbon Analyzer was used to measure the concentration of the fuel in the air. It works by automatically and continuously measuring the concentration of hydrocarbons in the sample. A regulated flow of sample is passed into a regulated hydrogen and helium flame. As the hydrocarbon sample is ionizable by the flame, there will be a flow of positive ions between two electrodes placed above the flame. The flow of ions causes current to flow through the internal electronic circuitry and the magnitude of this current is displayed on a counter installed on the cover. The current flow is proportional to the rate at which carbon atoms enter the flame. Therefore, it is an accurate measure of the concentration of the sample inlet. [23] A complete description and internal flow diagrams are shown in Appendix A2. This type of hydrocarbon analyzer is primarily used for low-level concentrations of hydrocarbons such as exhaust emissions from an internal combustion engine. Since these tests were of the motored engine type with no combustion, the FID had to be modified to accept the high levels of hydrocarbons. This model has dual-burner fuel capabilities; one for low concentration of hydrocarbons and the other for higher concentrations. The burner fuel, which allowed a higher concentration of carbon atoms to be read, was used. It consisted of 40% hydrogen and 60% helium, and it allowed a measurement of up to a 10% propane concentration. This change alone did not provide the necessary test range. A modification was made to increase flow resistance to reduce the flow rate of sample gas to the burner. This effectively reduced the concentration of the sample in the hydrogen and helium flame to an acceptable level for the FID. This modification also had the effect of increasing the response time, but it still was with

acceptable limits. To decrease the flow to the burner, the sample capillary tube length was increased. A 100 mm (3.937 in) length of 0.127 mm (0.005 in) capillary was installed with five small crimps in the tube. These crimps were made one at a time on a trial and test procedure to obtain the range that was needed at the fastest response time. When this was installed, two different span gases and a zero gas were used to verify that the response was linear. The sample from the intake manifold was delivered to the FID by way of a flow-rate controllable pumping station. This consisted of a rotometer and a four-way switch valve with a sample pump. The sample was delivered at a rate of 2.6 liters/minute to the sample inlet on the FID. Only a small portion of this sample is sent onto the burner, the remaining is bypassed to the exhaust. The switching valve was used for supplying nitrogen for a zero gas and a six-percent propane in nitrogen for a span gas. The span gas was supplied at the same rate as the sample to ensure accurate readings. The flame ionization detector and the pumping station are shown in Figure 14.

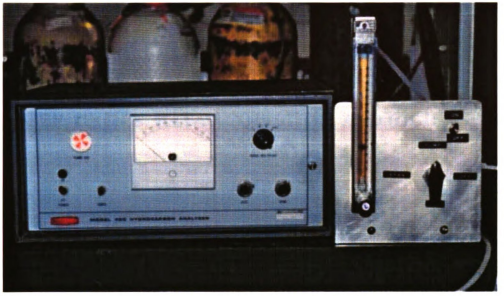

Figure 14. Flame Ionization Detector and Pumping Station

CHAPTER 3

LASER, OPTICS, DATA ACQUISTION, AND HIGH SPEED CAMERA

3.1 Laser and Optics

The general arrangement of laser, field-optics, and ICCD detector is shown in Figure 15. A Lambda Physik EMG 160 msc laser generated the excitation source for the LIF experiment. It was operated using xenon and hydrogen chloride gases, which provided an operating wavelength of 308 nm. The maximum power that was obtained for the tests was approximately 50 mJ/pulse. This laser produced a rectangular beam of 5 mm X 20 mm. Two pairs of cylindrical fused silica lenses formed the laser beam into a sheet of light 210-mm X 1.0 mm. All lenses were coated with anti-reflection coating to minimize losses. The relative transmittance of these lenses was 98%. Laser power was monitored by a Scitech Vector laser power/meter system. This power metering system consisted of a S200 single-channel, power and energy indicator, P25 25-mm pyro-electric detector, and VS25UV quartz, beam splitter. The beam splitter reflected 3.35 % of the beam into the detector and transmitted 82.5 %. [22] The sheet of light passed approximately 5mm below the cylinder head across the cylinders long axis. The

fluorescence image was directed down through the quartz piston and onto a mirror mounted at a 45-degree angle to the axis of piston motion. The mirror was of elliptic shape with major and minor axes of 66.68 mm (2.625 in) X 94.28 mm (3.712 in). The directed fluorescence was captured by a quartz camera lens (Nikkor UV lens, 50mm, f/11) attached to an Intensified Charged Coupled Device (ICCD) camera. To assure that only the fluorescence from the 3-Pentanone was obtained two band pass filters were used. The first band pass filter (CG-WG-345) turned on at 345nm and the other turned off (SWP-600) at 600nm. The data acquisition system was a Princeton Instruments digital, computer-controlled image acquisition system with a gated image intensifier. This camera has a high dynamic range, low noise, wide spectral sensitivity, adjustable gain, and adjustable electronic gating. The detector was a model ICCD-576 G/RB with a pixel array of 576 X 384, which was controlled by a model ST-130 controller. A FG-100 pulse generator provided the high voltage to the intensifier. The images were processed on a Gateway G6-180 Pentium Pro computer using CSMA software. False-color processing in which an assigned color corresponds to an intensity range was used for image enhancement. In all of the tests the laser and camera gate were electronically synchronized to allow the data acquisition in any part of the engine cycle. Fluorescence intensity was calculated the same for all test conditions. In all cases the intensities were averaged from ten individual images and normalized with laser energy. A region of interest in the beam was chosen and kept constant for all tests. Background images were taken first then raw data images followed. The averaged data images were then subtracted from the averaged background images and the data plotted.

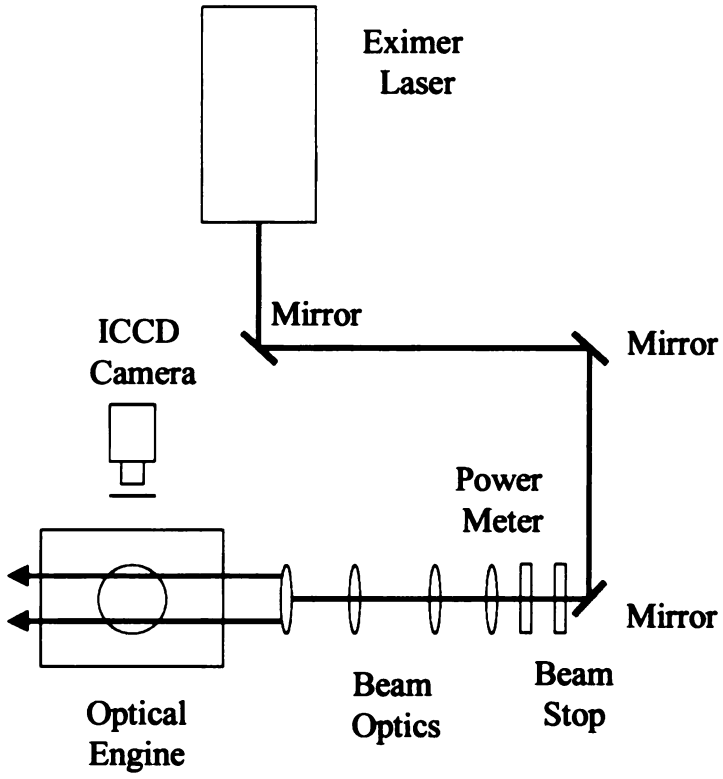

Figure 15. Laser, Beam Optics, and ICCD Camera Setup

3.2 Pressure Measurement

In-cylinder pressure measurements were made using a Kistler piezo-electric pressure sensor. This was mounted in the cylinder head by means of a threaded hole that was located between the two intake ports. The charge output was coupled to a Kistler amplifier and then to a data acquisition system. The data acquisition system was a RT Cam Real Time Combustion Analysis Module. Figure 16 shows a typical pressure trace of the optical engine operating at 600 rpm and wide-open throttle.

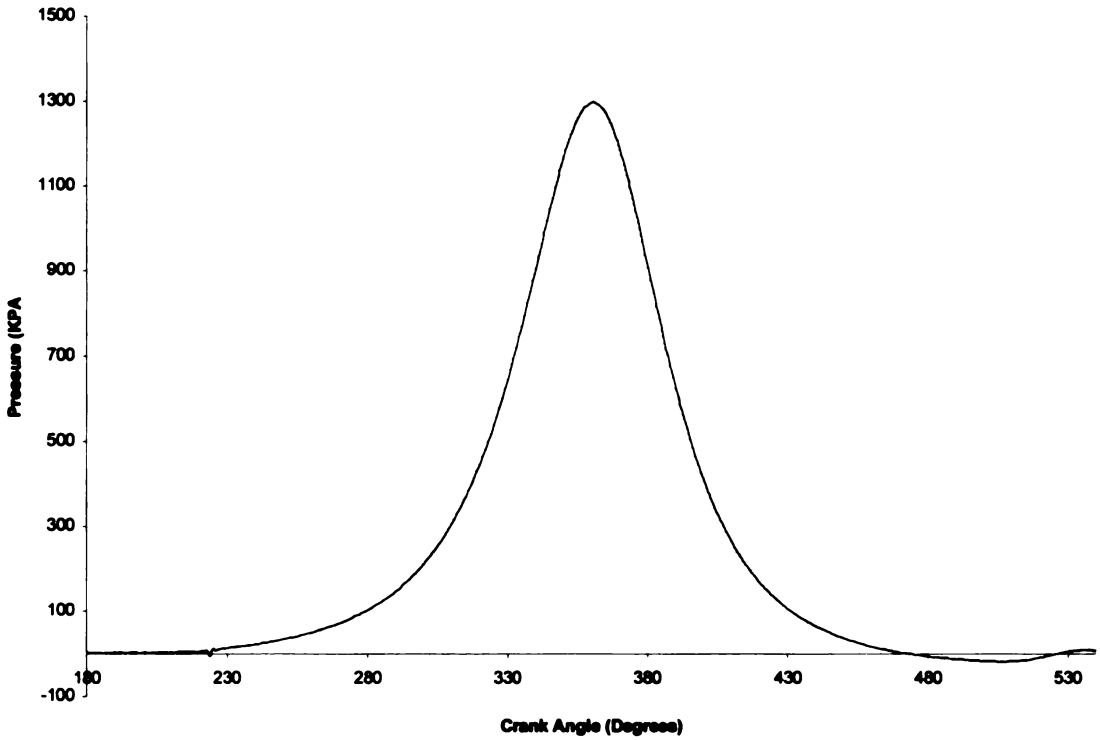

Figure 16. In Cylinder Pressure vs. Crank Angle

3.3 High Speed Camera and Copper Vapor Laser

A high-speed camera, model 370-35 rotating drum camera manufactured by Cordin, was used to obtain Mie scattering images in the optical engine. This camera has two modes of operation: a framing mode and a streak mode. The latter was used for this experiment. This works by bring the camera drum up to speed and opening shutter, pulsing the laser then after one rotation of the drum the shutter was electronically closed. The camera uses a one-meter strip of 35-mm film rotating at 200 revolutions a second. Since there is not enough room light scattered from the fuel spray to obtain a picture, an additional light source is

needed. This was provided by an Oxford Copper Vapor Laser, Model number ACL 45. The laser is fitted with an unstable resonator, which produces a beam with low divergence. The light that is produced is green with a wavelength in the range of 510.6 to 578.2 nm with an output of approximately 30 watts. This light was focused into a flat sheet of light approximately 5-cm wide by 3-mm thick. This type of laser is a pulse laser, so a synchronizing system between the camera and laser was used. In operation, the room lights were shut off. The shutter was opened electronically on the camera at a predetermined crank angle and the laser pulsed a set number of times then the shutter closed. For this configuration the laser pulsed 50 times, which corresponds to 50 half size 35-mm images on the film. The system configuration is in Figure 17.

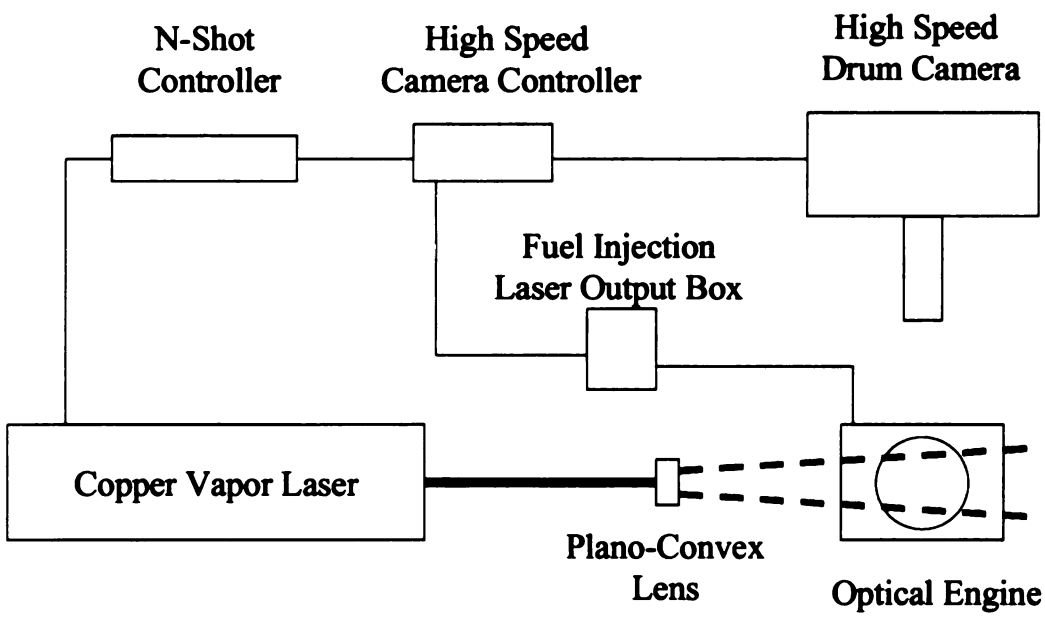

Figure 17. Schematic of High Speed Drum Camera Setup

CHAPTER 4

RESULTS AND DISCUSSION

4.1 Experimental Setup Results

4.1.1 Orifice Calibration

In order to determine the flow rate of fuel into the premixing system, the fuel flow rate metering orifices needed to be calibrated. This was accomplished by maintaining a constant pressure drop across the orifice using the pressurized fuel system of the premixing system. Figure 18 shows the flow rate through the orifice versus pressure drop for the four orifices. These curves were used to construct look up tables that were used during the flame ionization detector calibration and in the in-cylinder calibration.

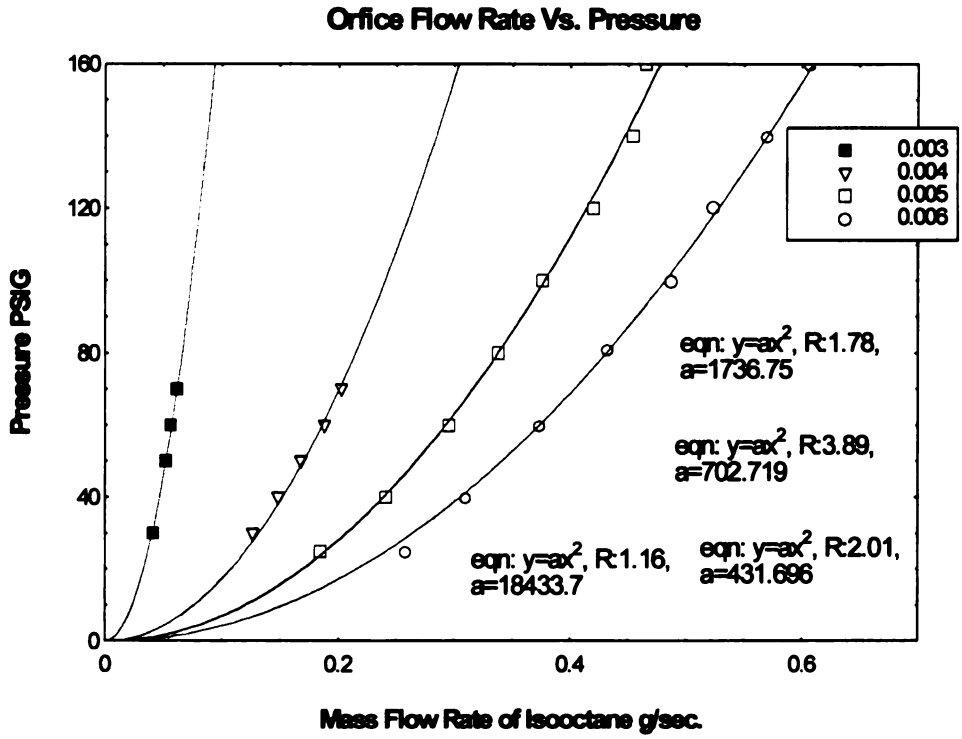

Figure 18. Orifice Flow Rate vs. Pressure Drop

4.1.2 Flame Ionization Detector versus Measured Equivalence Ratio

A modified FID was used to verify the measured equivalence ratio of the premixing system. The FID was calibrated first using nitrogen for the zero gas then eight-percent propane in nitrogen for the span gas. Since the response of the FID is linear, only these two points were needed for self-calibration [23]. The premixing system was started, and the mass flow rate of nitrogen or air was measured by the laminar flow element. The mass flow rate of the fuel was established, given an orifice size and pressure drop across the orifice, from the orifice calibration. After correcting the mass flow rate of nitrogen or air for the inlet temperature and pressure, the measured equivalence ratio was calculated and compared with the FID. The output of the FID was via analog scale on the front of the FID, which measures amperes. These numbers, corresponding to individual carbon atoms, were then converted to a percentage of carbon atoms and then to an equivalence ratio. These two different methods of obtaining the delivered equivalence ratio were compared for 100% isooctane and are shown in Figure 19. The results show no more than a 4% error in agreement. A mixture of 3-pentanone, 40% by mass, in iso-octane did not show such good agreement. The discrepancy was in the range of 30%. This is shown in Figure 20. It is most likely due to not all of the carbon atoms being ionized. The accepted way of determining the response factor for the FID to correct for this is by the effective carbon number method, which was employed in these experiments [23, 24]. The error in this method of determining carbon numbers in mixtures is $\pm$ 10%, which when added to the error for isooctane and 3-pentanone alone would account for the larger error for the mixture. A complete description of the response of the FID using the effective carbon number is in appendix A2. For the in-cylinder

calibration, equivalence ratio calculated from air flow and pressure drop measurements was used. The FID was used as an indicator to assure the system was functioning properly. As long as the error was within the 30% range for the FID when using the 40% 3-pentanone mixture the premixing intake system was assumed to be functioning correctly.

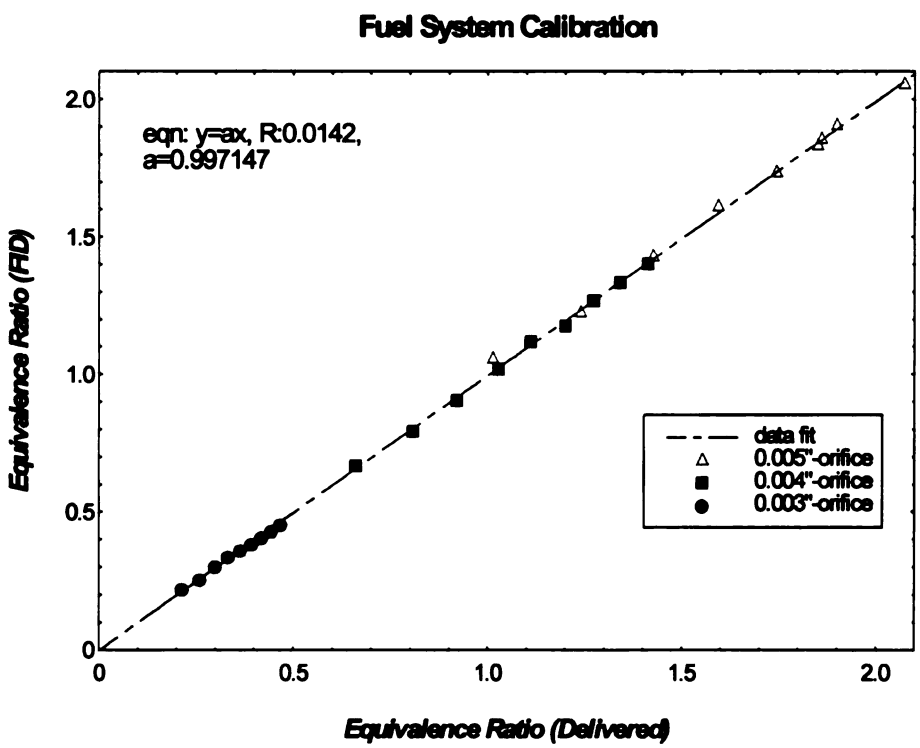

Figure 19. Equivalence Ratio Calculated from Direct Measurements of Nitrogen and Fuel Flow vs. Equivalence Ratio Obtained from Flame Ionization Detector Using 100% Isooctane

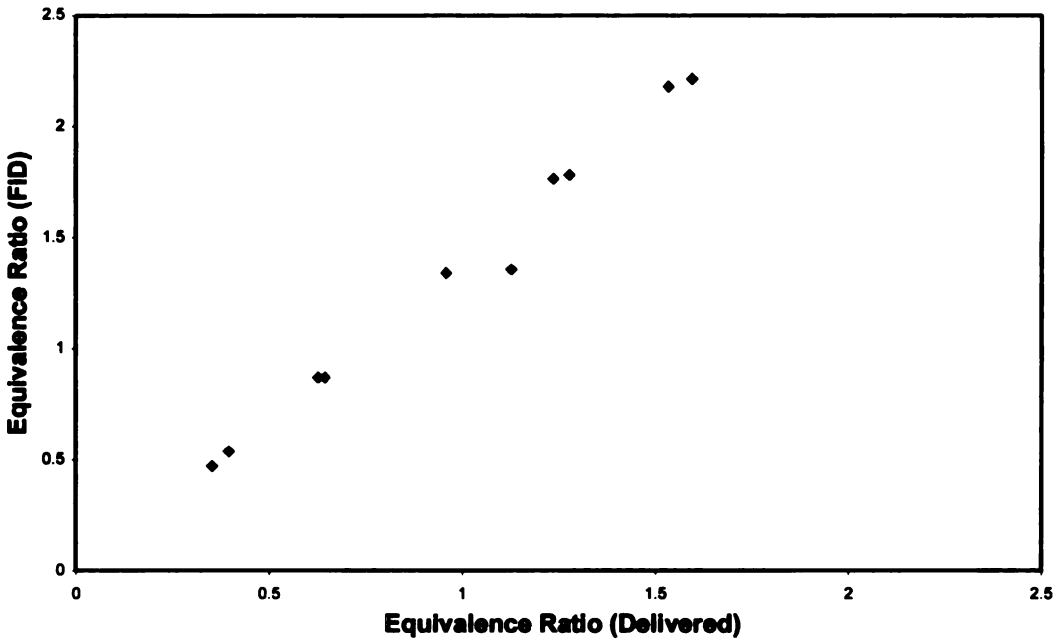

Figure 20. Equivalence Ratio Calculated from Direct Measurements of Nitrogen and Fuel Flow vs. Equivalence Ratio Obtained from Flame Ionization Detector Using 40% 3-Pentanone in Isooctane

4.1.3 In Cylinder Calibration

Laser induced fluorescence allows us to obtain two-dimensional images of the fuel distribution in the cylinder of the optical accessible engine. These images without calibration are only qualitative. To make such images quantitative, there is a need for an in-cylinder calibration to account for the temperature and pressure effects in the

environment a reciprocating engine. This type of calibration also takes into account the laser beam length and the curvature of the quartz cylinder. The laser beam passed through the quartz cylinder approximately 5 mm below the cylinder head and between the exhaust and intake valves. Figure (21) shows the position of the laser sheet and the area in which the average intensity was calculated. The dashed box shows this area of interest.

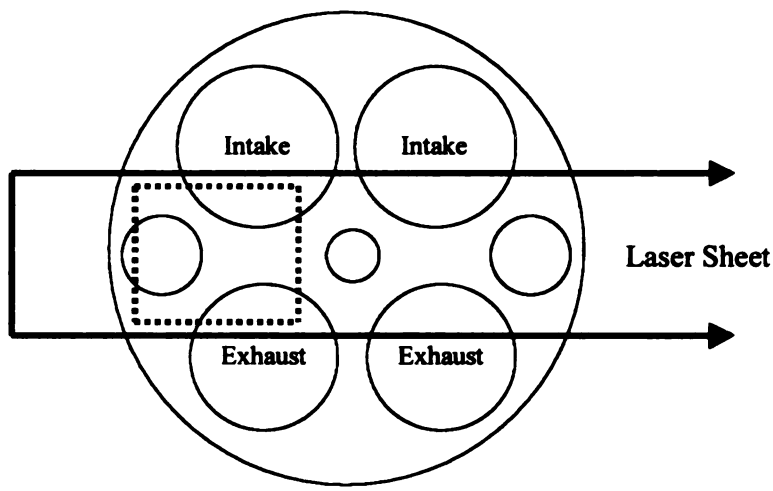

Figure 21. Laser Sheet and Area of Interest for Data Acquisition

Nitrogen was used to ensure safety during initial runs and to eliminate any of the oxygen quenching effects of the 3-pentanone. The oxygen quenching effects were known to be small, but were verified using this experimental setup [8-11]. To obtain a base line for the LIF intensity, a 100% solution of 3-pentanone was used. Background

images with no fuel were first taken and then subtracted from the raw images. The images were taken at each crank angle and were an average of 10 individual images. The equivalence ratio was kept constant and the laser and camera delay were changed to obtain data at different crank angles. The engine speed was 600 rpm with a wide-open throttle condition. Figure 22 shows that the intensity increased linearly as the equivalence ratio was increased. This is expected since the intensity is directly related to the quantity of chemical. Figure 23 shows that the intensity was constant for the duration of the intake stroke, because the in-cylinder pressure remains constant. The intensity increased during the compression stroke at the same rate as the volume in the cylinder decreased. This increase in intensity can be attributed to the decrease in the effective volume, thereby increasing the density of 3-pentanone, which is directly related to the intensity. These results allowed a base line to be formed from the optimum conditions: nitrogen environment and 100% fluorescing chemical. The lowest amount of fluorescing chemical that could be used for an acceptable signal to noise ratio was found to be a mixture of 40% by mass of 3-pentanone in 60% isooctane. This was found by starting with 10% 3-pentanone mixture then testing. The concentration was then increased in 10% increments until an acceptable signal to noise ratio was found.

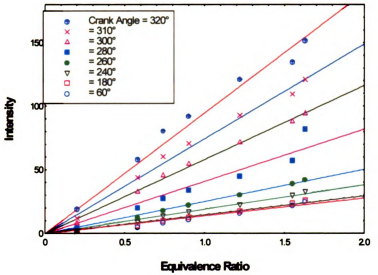

Figure 22. Equivalence Ratio vs. Intensity for 100% 3-Pentanone in a Nitrogen Environment

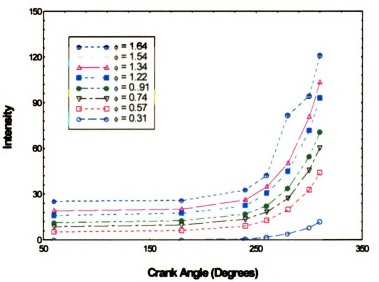

Figure 23. Crank Angle vs. Intensity for 100% 3-Pentanone in a Nitrogen Environment

The next series of tests used 40% 3-pentanone in isooctane and a nitrogen environment. Figures 24 and 25 show these results, which are similar to the 100% 3-pentanone case previously discussed. The intensity increased with decreasing volume and the intensity increased linearly with increasing equivalence ratio. It can also be shown that the effect of self-quenching was small on 3-pentanone with no more that 10% reduction in expected intensity from the 100% 3-pentanone case. Experiments were then conducted again using the same 40% 3-pentanone in isooctane, but air was used as the environment to determine the effects of oxygen quenching. Figure 26 and 27 show crank angle versus intensity and equivalence ratio versus intensity. These figures show similar trends with the previous results. The intensity increased linearly with the increased equivalence ratio and the intensity increased with decreasing volume.

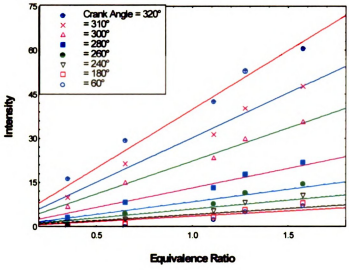

Figure 24. Equivalence Ratio vs. Intensity for 40% 3-Pentanone in a Nitrogen Environment

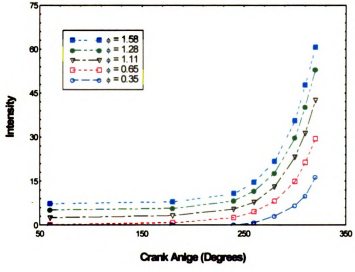

Figure 25. Crank Angle vs. Intensity for 40% 3-Pentanone in a Nitrogen Environment

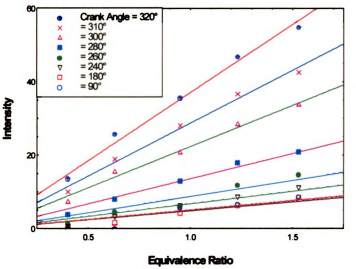

Figure 26. Equivalence Ratio vs. Intensity for 40% 3-Pentanone in an Air Environment

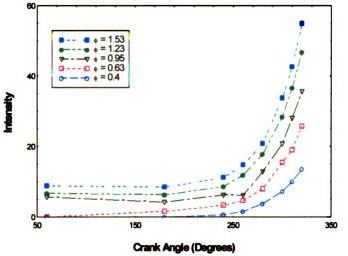

Figure 27. Crank Angle vs. Intensity for 40% 3-Pentanone in an Air Environment

The intensity was plotted against the average in-cylinder pressure at the given crank angle. These plots are shown in Figures 28 and 29. Figure 28 shows results that were conducted in a nitrogen environment and Figure 29 shows results that were conducted in an air environment. Both figures show some effect on the intensities with increasing pressure. Fujikawa et al. [13] performed pressure dependence experiments of 3-pentanone in a constant volume vessel. These tests were conducted at an excitation wavelength of 248 nm and 266 nm. The results revealed a low-pressure dependence of 3-pentanone. The excitation wavelength used in the present experiments was 308 nm; but if the same pressure dependence is assumed, then the LIF intensity should vary linearly with pressure. Aside from pressure dependence, possible reasons for this deviation may be due to blow-by past the piston rings or temperature effects. The effect of oxygen quenching was evident with a slight reduction in intensity. It was found to be about 20% for low equivalence ratios and around 10% for the upper end of equivalence ratios. This was calculated by using interpolation from the curve fits on figures 28 and 29.

Figures 30 through 35 show the beam passing through the optical engine with the premixing system providing an equivalence ratio of 1.6 and different crank angles. The slight variations in the intensity across the beam width are attributed to a build up of chemicals on the combustion chamber. This is evident with high intensity regions which, correspond to valve edges, injector tip and spark plug tips. Highest intensity areas seemed to be on the right side of the combustion chamber when viewing up through the quartz piston. Because of this, the area of interest for obtaining an average intensity was a box on the left side of the beam. These images also verified the function of the premixing system to produce a homogenous mixture of air and fuel.

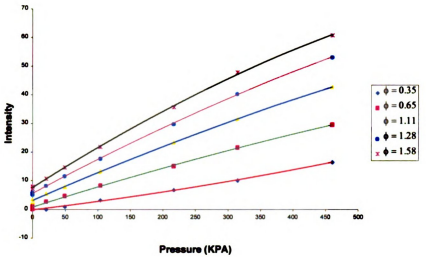

Figure 28. Pressure vs. Intensity 40% 3-Pentanone in Nitrogen Environment

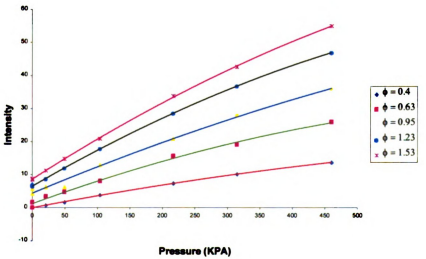

Figure 29. Pressure vs. Intensity 40% 3-Pentanone in Air Environment

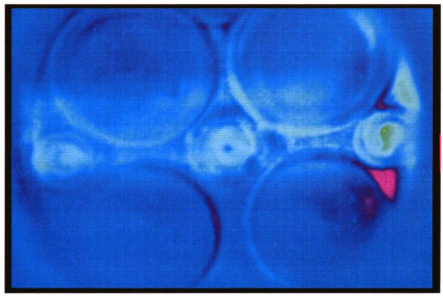

Figure 30. Laser Induced Fluorescence Calibration Image, Equivalence Ratio of 1.6, 260° After Top Dead Center Intake

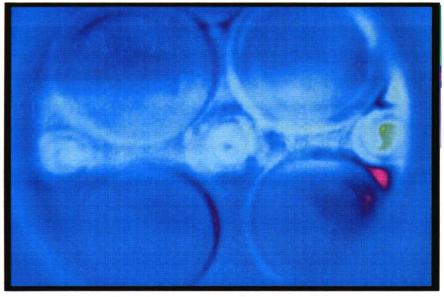

Figure 31. Laser Induced Fluorescence Calibration Image, Equivalence Ratio of 1.6, 260° After Top Dead Center Intake

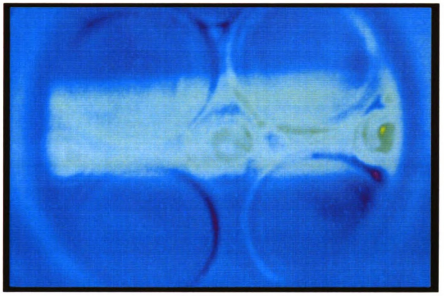

Figure 32. Laser Induced Fluorescence Calibration Image, Equivalence Ratio of 1.6, 280° After Top Dead Center Intake

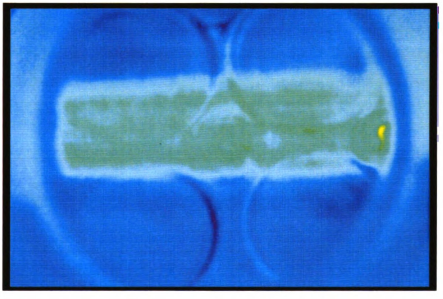

Figure 33. Laser Induced Fluorescence Calibration Image, Equivalence Ratio of 1.6, 300° After Top Dead Center Intake

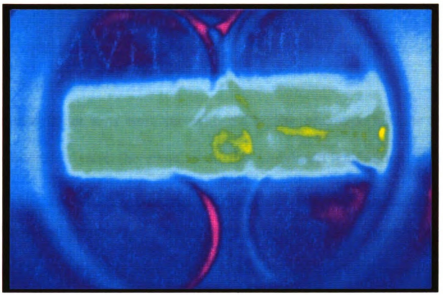

Figure 34. Laser Induced Fluorescence Calibration Image, Equivalence Ratio of 1.6, 310° After Top Dead Center Intake

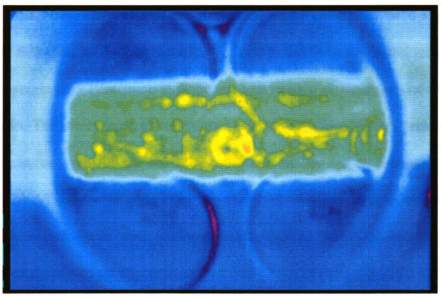

Figure 35. Laser Induced Fluorescence Calibration Image, Equivalence Ratio of 1.6, 320° After Top Dead Center Intake

4.2 In-Cylinder Results

The in-cylinder tests were run with a Chrysler prototype injector and cylinder head. All conditions were the same as in the in-cylinder calibration. Four different timings and injector pressures were examined: an early injection with a timing of 120 ATDC and two fuel pressures of 400 psi and 1000 psi and a late injection with a timing of 240 ATDC and the same fuel pressures. These conditions serve as a test to measure the mixing of the air and fuel mixture in the cylinder under different conditions and to verify the technique is applicable for these conditions.

4.2.1 Direct Injection Tests

The direct injection tests were run at the same conditions as the calibrations, which were 600-rpm, wide-open throttle. As was found from the initial tests, a mixture of 40% by weight of 3-Pentanone in isooctane was needed to obtain an acceptable signal to noise ratio. The direct injection tests used a prototype Chysler high-pressure injector. The fuel pressures were 400 psi and 1000 psi with a duration of 1.17 ms and an injection timing of 120 ATDC for an early injection and 240 ATDC for a late injection. Timing earlier and later than these crank angles created problems with contaminating the piston top. The laser sheet was set approximately 5 mm below the bottom of the cylinder head, which permitted the viewing of images up to 320 degrees ATDC. Figures 36 and 37 show in-cylinder images were injection starts at 120 ATDC. The bar graph at the bottom of the figure represents varying equivalence ratios. These values were calculated by

reading in the ASCII file from the CSMA software to a special program. These values were then converted from an intensity value to an equivalence ratio by using the best-fit curve from the calibration. Figure 36, which shows a condition of 400 psi and 1.17 ms duration, shows a region of uniformly mixed fuel in the cylinder but an overall low equivalence ratio with a maximum less than 0.5. Figure 37, which has a 1000 psi and 1.17 ms duration, shows a high concentration of fuel of approximately 1.21 equivalence ratio in the center of the cylinder and steadily decreasing to the edge of the cylinder. This distribution of fuel could possibly cause ignition problems since this cylinder head has two spark plugs, both of which are on the periphery of the combustion chamber. Figures 38 and 39 show a late-injection condition with the start of injection at 240 ATDC. Figure 38 has similar results to Figure 37 with a high concentration of fuel in the center of approximately 0.81 equivalence ratio and diminishing outward towards the cylinder wall. Figure 39 show a ringed pattern with high concentrations on the left. This is most likely due to liquid fuel coming in contact with the piston top and contaminating it. Because of this contamination obtaining any usable results was not possible at these late timings and high pressures. Figure 40 shows the following four images using the same equivalence ratio range to show the large changes in the mixture composition from case to case.

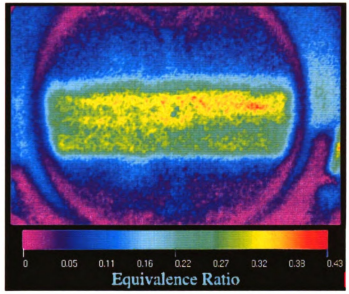

Figure 36. Laser Induced Fluorescence of Direct Injection at 320° After Top Dead Center Intake, Start Of Injection 120° After Top Dead Center Intake, Fuel Pressure 400 psi

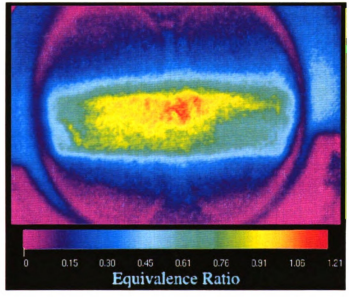

Figure 37. Laser Induced Fluorescence of Direct Injection at 320° After Top Dead Center Intake, Start Of Injection 120° After Top Dead Center, Fuel Pressure 1000 psi

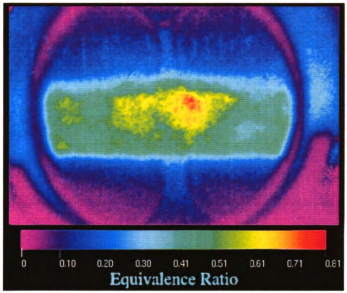

Figure 38. Laser Induced Fluorescence of Direct Injection at 320° After Top Dead Center Intake, Start Of Injection 240° After Top Dead Center, Fuel Pressure 400 psi

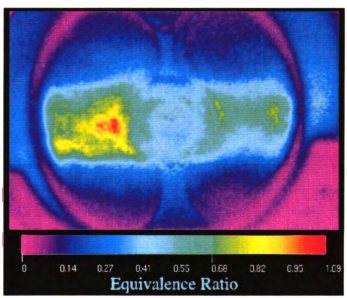

Figure 39. Laser Induced Fluorescence of Direct Injection at 320° After Top Dead Center Intake, Start Of Injection 240° After Top Dead Center, Fuel Pressure 1000 psi

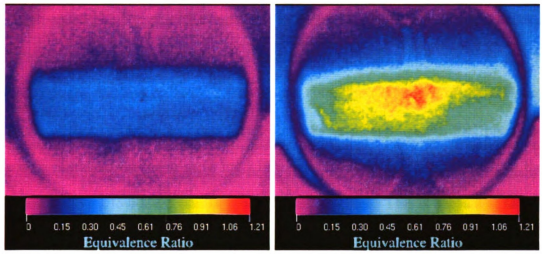

S.O.I. 120° ATDCI
Fuel Pressure 400 psi

S.O.I. 120° ATDCI
Fuel Pressure 1000 psi

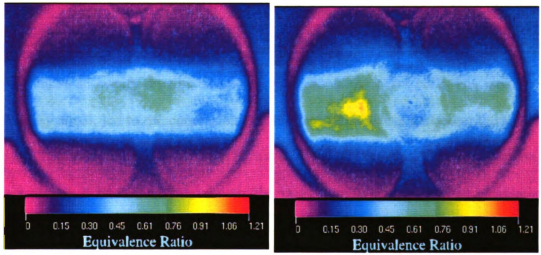

S.O.I. 240° ATDCI
Fuel Pressure 400 psi

S.O.I. 240° ATDCI
Fuel Pressure 1000 psi

Figure 40. Laser Induced Fluorescence of Direct Injection at 320° After Top Dead Center

4.2.2 High Speed Flow Visualization Using Mie Scattering

High-speed photography Mie scattering light from a copper vapor laser was used to determine if there was any liquid fuel droplets in the cylinder. This experiment was conducted to indicate if the calibration was usable, since the calibration of the LIF was based on all of the fuel being in vapor form. The data acquisition times, fuel pressures and duration remained the same as in the LIF experiments. It should be noted that the figures should show a low-level intensity in the optimum cases. This is because if all the fuel is in vapor form there are no liquid fuel droplets to scatter the light. Figures 41 and 42 show the images of an early injection timing of 120° ATDC. Figure 41, which is the low-pressure case of 400 psi and shows no scattering at all. This is most likely due to the small quantity of fuel being injected, all of which is evaporated, which results in a very lean mixture. This was also shown in the LIF image, Figure 36, which shows a maximum equivalence ratio of only 0.43. Figure 42, which is the high-pressure case of 1000 psi, shows an evenly distributed scattering region in the beam path. The intensity, which is very small, led to the conclusion that the particles that are scattering light must be vapor. The scattered light may also be water vapor since the experiment was done using air. Previous experience has shown that water vapor appears on the expansion stroke. Figures 43 and 44 show the late injection case of 240° ATDC. Figure 43 shows the low-pressure case. It can be seen that on the right hand side of the image there is a region that has a slightly higher intensity, which may be small liquid droplets. Other scattering pictures that were obtained just after injection showed very high intensities. These high intensity regions correspond liquid droplets. This high intensity liquid scattering can be seen in Figure 45. This shows an injection timing of 280° ATDC with

the image taken at 285° ATDC. Images takes within a few degrees after injection can be assumed to contain liquid. This image was used as a reference for intensities of liquid scattering. Since none of the prior images showed similarly high intensities, the calibration of vapor only is a reasonable assumption for laser induce fluorescence.

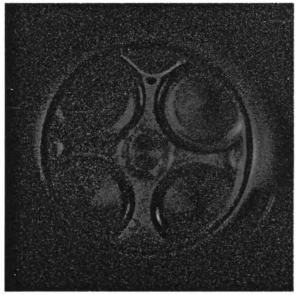

Figure 41. Mie Scattering of Direct Injection at 320° After Top Dead Center Intake, Start Of Injection 120° After Top Dead Center, Fuel Pressure 400 psi

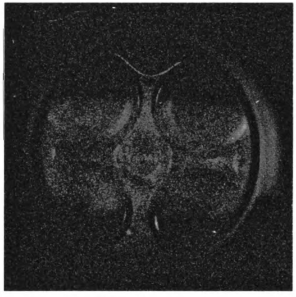

Figure 42. Mie Scattering of Direct Injection at 320° After Top Dead Center Intake, Start Of Injection 120° After Top Dead Center, Fuel Pressure 1000 psi

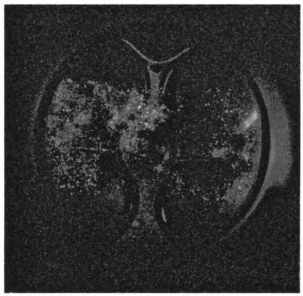

Figure 43. Mie Scattering of Direct Injection at 320° After Top Dead Center Intake, Start Of Injection 240° After Top Dead Center, Fuel Pressure 400 psi

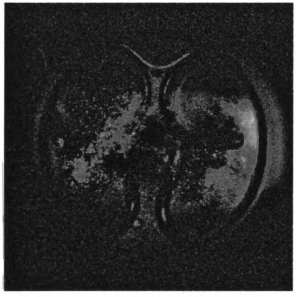

Figure 44. Mie Scattering of Direct Injection at 320° After Top Dead Center Intake, Start Of Injection 240° After Top Dead Center, Fuel Pressure 1000 psi

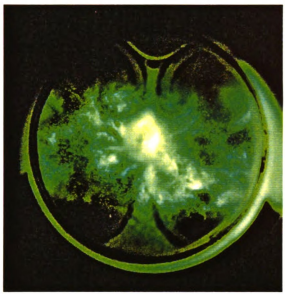

Figure 45. Mie Scattering of Direct Injection at 285° After Top Dead Center Intake, Start Of Injection 280° After Top Dead Center, Fuel Pressure 1000 psi

CHAPTER 5

SUMMARY AND CONCLUSIONS

1. The optically accessible motored engine constructed for LIF studies and high-speed photography provided the optical access necessary to accomplish an extensive in-cylinder analysis of the engine.

2. The premixing intake system designed and constructed as part of this work was capable of providing a known concentration of fuel and air or nitrogen to the motored engine

3. The use of 3-pentanone is a good choice for a chemical tracer for isooctane in an oxygen environment, such as an internal combustion engine.

4. There is a need for an extensive in-cylinder calibration of the type that was performed in this experimental study if accurate quantifiable results are to be expected. This should include a flow visualization to determine if liquid fuel is present.

5. A low concentration hydrocarbon analyzer can be used to measure high levels of hydrocarbons if used according to the methods described in this work.

6. The effect of self-quenching on 3-pentanone is less than 10%.

7. The effect of oxygen quenching on 3-pentanone for a sample case of $\phi = 0.5$ showed a maximum of 20% reduction in intensity and a sample case of $\phi = 1.4$ showed a reduction in intensity of 10%.

8. The use of laser induced fluorescence for obtaining quantitative fuel distribution information in an optically accessible directly injected engine of this type has limitations especially for late-injection and high-pressure timings because of liquid pooling on the quartz piston crown.

9. The use of Mie scattering in conjunction with laser induced fluorescence experiments proves a useful auxiliary method for studying mixing and evaporation processes in an internal combustion engine.

CHAPTER 6

RECOMMENDATIONS

1. The use of an excitation wavelength nearer the peak of the absorption spectrum of 3-pentanone may increase the signal to noise ratio and allow a lower concentration of tracer to be used.

2. If the current Eximer laser is to be used for future experiments, it should be moved in a more direct path, or laser power increased, to provide more available energy to excite LIF chemicals.

3. The intake plenum should be modified to withstand vacuum conditions for part-throttled conditions.

4. An exciplex system would be superior to the single-phase 3-pentanone system and needs further development.

5. The temperature effects of 3-pentanone in a motored engine need to be investigated.

6. A device should be added to the fuel injector control box, which would trigger the injector once, then cycle a set number of times, then trigger again. This would help to reduce the build-up of liquid layers on the piston, cylinder and combustion chamber.

LIST OF REFERENCES

LIST OF REFERENCES

1. Melton, L. A., "Spectrally separated fluorescence emissions for diesel droplets and vapor", Applied Optics, Vol. 22, No. 14, pp. 2224-2226, 1983.

2. Hale, S. J. and Melton L. A., "Absolute Quantum Yields for Exciplex Fluorescence", Applied Spectroscopy, Vol. 44, No. 1, pp. 101-105, 1990.

3. Kim J. U., Golding B., Schock H., Keller P., Nocera D., "Exciplex Fluorescence Visualization System for Pre-Combustion Diagnosis of an Automotive Gasoline Engine", SAE Paper 960826, 1996.

4. Kim, "Visualization of Two-Phased Fluid Distributions Using Laser-Induced Exciplex Fluorescence", Ph. D. Dissertation, Physics, Michigan State University, 1997.

5. Shimizu, R., Matumoto, S., Furuno, S., Murayama, M. and Kojima, S., "Measurement of Air-Fuel Mixture Distribution in a Gasoline Engine Using LIEF Technique", SAE Paper 922356, 1992.

6. Kim, K. S., Choi, M. S., Lee, C.H. and Kim, W. T., "In-Cylinder Fuel Distribution Measurements Using PLIF in a SI Engine", SAE Paper 970509, 1997.

7. Fansler, T., French, D. and Drake, M., "Fuel Distributions in a Firing Direct-Injection Spark-Ignition Engine Using Laser-Induced Fluorescence Imaging", SAE Paper 950110, 1995.

8. Johansson, B., Neij, H., Alden, M. and Juhlin, G., "Investigations of the Influence of Mixture Preparation on Cyclic Variations in a SI-Engine, Using Laser Induced Fluorescence", SAE Paper 950108, 1995.

9. Lawrenz, W., Kohler, J., Meier, F., Stolz, W., Wirth, R., Bloss, W. H., Maly, R. R., Wagner, E. and Zahn, M., "Quantitative 2D LIF Measurements of Air/Fuel Ratios During the Intake Stroke in a Transparent SI Engine", SAE Paper 922320, 1992.

10. Berckmuller, M., Tait, N. P, Lockett, R. D., Greenhalgh, D. A., Ishii, K., Urata, Y., Umiyama, H. and Yoshida, K., "In-Cylinder Crank-Angle-Resolved Imaging of Fuel Concentration in a Firing Spark-Ignition Engine Using Planar Laser-Induced Fluorescence", Twenty-Fifth Symposium (International) on Combustion/The Combustion Institute, pp. 151-156, 1994.

11. Neij, H., Johansson, B. and Alden, M., "Development and Demonstration of 2D-LIF for Studies of Mixture Preparation in SI Engines", Combustion and Flame, Vol. 99, pp. 449-457, 1994.

12. Bowditch, F. "Combustion Problems in Gasoline Engines", Research Laboratories, General Motors Corporation Warren, Michigan, 1960.

13. Fujikawa, T., Hattori, Y. and Akihama, K., "Quantitative 2-D Fuel Distribution Measurements in an SI Engine Using Laser-Induced Fluorescence with Suitable Combination of Fluorescence Tracer and Excitation Wavelength", SAE Paper 972944, 1997.

14. Berckmuller, M., Tait, N. P. and Greenhalgh, D. A., "The Time History of the Mixture Formation Process in a Lean Burn Stratified-Charge Engine", SAE Paper 961929, 1996.

15. Tabata, M., Kataoka, M., Fujimoto, M. and Noh, Y., "In-Cylinder Fuel Distribution, Flow Field, and Combustion Characteristics of a Mixture Injected SI Engine", SAE Paper 950104, 1995.

16. Alberty, R., 1983, "Physical Chemistry", John Wiley and Sons, New York.

17. Hansen, A. D. and Lee, E., "Radiative and nonradiative transitions in the first excited singlet state of symmetrical methyl – substituted acetones", The Journal of Chemical Physics, Vol. 62, No. 1,
pp. 183-189, 1975.

18. Grossmann, F., Monkhouse, P.B., Ridder, M., Sick, V. and Wolfrum, J., "Temperature and pressure dependence of the laser-induced fluorescence of gas-phase acetone and 3-pentatnone", Appl. Phys. B, Vol. 62, pp. 249-253, 1996.

19. Smith, B. and Srivastava, R. 1986, " Thermodyanamic Data For Pure Compounds", Part A Hydrocarbons and Ketones, Elsevier Science Publishing Company Inc., New York.

20. Moldex Cranks, 25229 West Warren Dearborn Heights MI, 48127-2148.

21. Taylor, C. F. 1986. "The Internal Combustion Engine in Theory and Practice", Volume 2. Massachusetts Institute of Technology, Massachusetts.

22. Schafer R. "The Development of an Improved Quantitative Calibration for an Exciplex Liquid/Vapor Fuel Visualization System", Masters Thesis, Michigan State University, 1993.

23. "Instruction Manual," Beckman Model 400 Hydrocarbon Analyzer, 1970.

24. Private discussion with M. C. Drake, GM R&D Center.

25. Incropera, F., and De Witt, D., 1990. "Introduction to Heat Transfer", Jon Wiley and Sons, New York.

26. Cengel, Y. and Boles, M. 1989, "Thermodynamic: An Engineering Approach", McGraw-Hill, Inc., New York.

Appendix

Appendix

A.1 Heat transfer Analysis of the Intake System

A heat transfer analysis was carried out to determine the power needed for the air preheater and mixing-zone heating tape. The system was initially assembled and tested with low flow rates of nitrogen and fuel in order to obtain a base line from which to start. For a first approximation, this analysis only takes into account the convective heat transfer. Conduction and radiation are assumed to be zero. Figure A1 shows the schematic of the complete premixing intake system. Flow through the pipe was first calculated and found to be turbulent using equation (A1). The mass flow rate of nitrogen for the 600-rpm wide open throttle condition, which was 5.5 SCFM, was used. The Reynolds number was calculated to be 6400. Flow in a pipe with a Reynolds number higher than 2300 is assumed to be turbulent [25].

$$\mathrm{Re}_d = \frac{4\dot{m}}{\pi D \mu} \tag{A1}$$

A control volume approach was used for the mixing zone region. Preheated nitrogen and liquid fuel entered and fuel vapor and nitrogen exited. This can be seen in Figure A2.

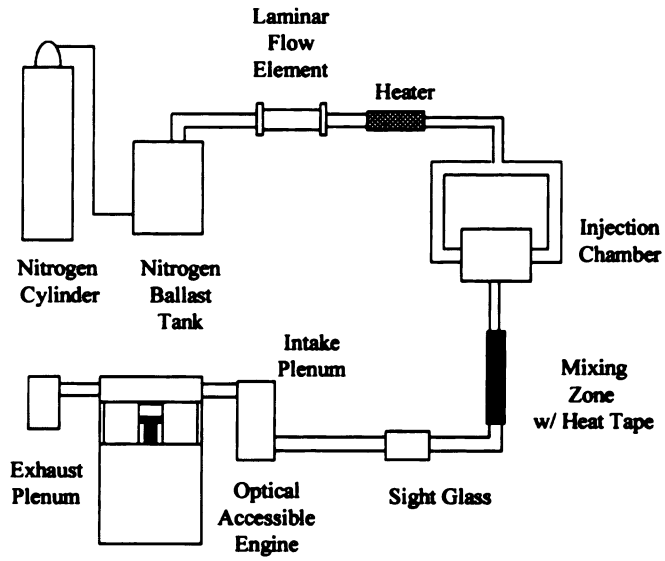

Figure A1. Schematic of Premixing Intake System

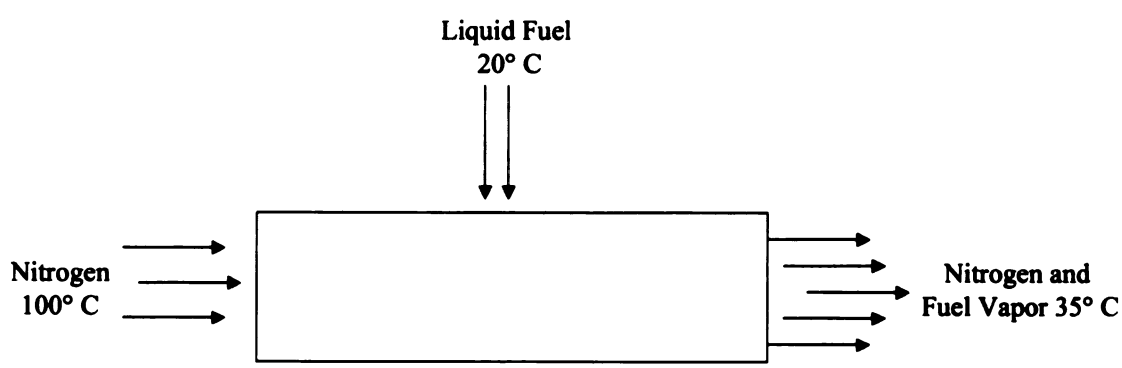

Figure A2. Premixing System Mixing Zone

The fuel flow rate that was used for the calculations was the maximum amount of fuel that would be used during the experiment. This was 0.45 g/sec., which corresponds to an equivalence ratio of 2.0 at 5.5 SCFM. The heat of vaporization for isooctane was found to be 35134 J/mole @ 299K [26]. Using the flow rate of fuel for the maximum condition, the energy needed to evaporate the liquid fuel was calculated to be 112 watts.

Applying the conservation of energy to the control volume, it is assumed that the rate of convective heat transfer to the fluid inside the pipe must equal the rate at which thermal energy is added to the system. Making these assumptions equation (A2) for the head transfer to the working fluid can be used.

$$q_{conv} = \dot{m} c_p (T_{m,o} - T_{m,i}) \qquad \text{(A2)}$$

Using equation 4 the heat transfer rate of the preheated nitrogen was calculated to be 210 Watts in the mixing zone, where it's temperature was reduced from 100° C to 35° C. The amount of power needed to raise the fuel vapor from 20° C to 35° C at this flow rate was calculated to be 13.23 Watts. Heating tape was used in the mixing zone to raise the surface temperature of the wire mesh. This provided a hot surface upon which the liquid fuel droplets could impinge and evaporate. This heating tape was run at 50 volts and 2.7 amperes and produced 135 watts.

The overall energy balance was calculated as follows. The heat of vaporization of the liquid fuel at the desired flow rate was 112 W. The power required to raise the temperature of the fuel vapor was 13.23 W. The total power to vaporize and raise the temperature of the liquid fuel was 125.23 W. The total energy provided to the system

was made up of preheated nitrogen, which gave up 210 W and the heating tape, which provided 135 W. This total power added to the system was then 345 W. This difference between the total power needed to evaporate and raise the temperature of the liquid fuel and the total power added to the system was 220 watts. This was attributed to the heat loss of the system. This is reasonable since some parts of the system were not insulated.

A.2 Flame Ionization Detector

A.2.1 Internal Schematic and Burner Diagram

Figure A3 shows a schematic of the internal parts and a flow diagram of the flame ionization detector. Adjustable pressure regulators are used on the sample, air and fuel inlet lines. The air and fuel pressure regulators control the pressure on the downstream side. The air and fuel pressure regulators were maintained at 20 psig. The sample regulator controlled pressure on the upstream side and was set to 2.5 psig. This also passed any excess gas through the by-pass outlet.

The burner schematic is shown in Figure A4. The sample and fuel gases enter the burner and travel to the burner jet. The air flows around the periphery of the burner. These two gases mix and burn in a diffusion flame at the tip of the burner jet. The burner jet and the collector form the electrodes for the ionization sensing. The burner jet forms the positive terminal and the collector form the negative terminal. The charged particles, (electrons and positive ions) which are formed by the combustion energy in the burner flame, are collected on the positive and negative terminals. The negatively charged electrons accumulate on the burner jet and the positive ions collect on the collector. This

flow of ions is what causes current to flow. The magnitude of this current is based on the concentration of carbon atoms in the sample. [23]

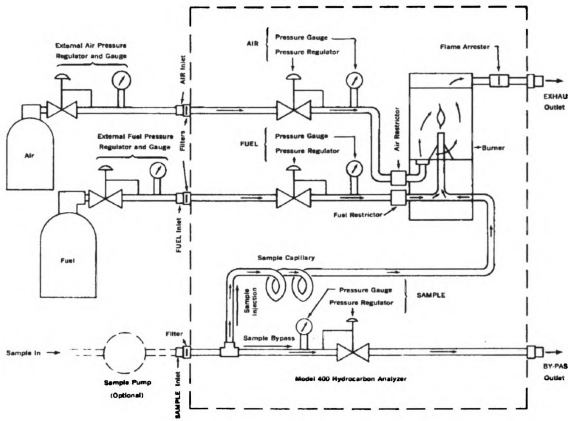

Figure A3. Flame Ionization Detector Internal Schematic [23]

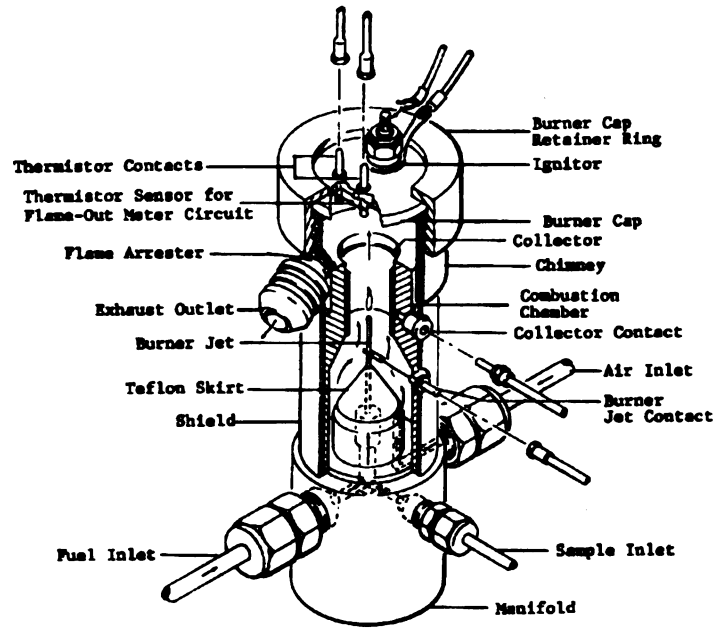

Figure A4. Flame Ionization Burner Assembly [23]

A.2.2 Flame Ionization Response Using the Effective Carbon Number

The response of the FID to changes in sample gas is due to changes in the number of carbon atoms being ionized. For simple carbon based molecules, such as propane which was used for the self-calibration, the ionization of the carbon atoms is complete. For some other molecules the ionization of the carbon is not complete because the carbon atoms are bonded to other molecules such as nitrogen and oxygen. Therefore an adjustment is needed when comparing molecules that are totally ionized and ones that are not. The response of an atom may be expressed *approximately* by a value designated the "effective carbon number" (ECN). The effective carbon number of a particular carbon atom is defined as the ratio between the instrument response caused by an atom of this type and the instrument response caused by an aliphatic carbon atom. For ketones such as

3-pentanone there is one carbon atom that is part of the carbonyl group which is already partially oxidized. The carbon atom in 3-pentanone has been found experimentally not to give a FID response signal. The ECN for 3-pentanone is therefore the number of carbon atoms minus one. [23, 24] Table A1 shows the different chemicals and their corresponding effective carbon numbers.

Table A1. Approximate Effective Carbon Numbers for the Compounds used with Flame Ionization Detector

Chemical Compound	Effective Carbon Number (ECN)
Propane (span gas) C_3H_8	3
3- Pentanone $C_5H_{10}O$	4
Isooctane C_8H_{18}	8

From Table A1 it can be seen that the response of pure isooctane is twice that of pure 3-pentanone base on the effective carbon number. The response factor can be calculated for the 40% 3-pentanone mixture in isooctane using these effective carbon numbers. This response factor is then used to adjust the output readings to compare with a pure substance. The response factor used in the experiment was calculated as in equation A3.

$$RF = 0.4(2) + 0.6(1) = 1.4 \qquad \text{A3}$$

These effective carbon numbers have been found experimentally and can only be expected to have an accuracy in the range of $\pm$ 10%. Therefore the use of the FID for this study was to act as an indicator of the functioning of the premixing intake system.

A 30% disagreement was found when using a 40% 3-pentanone in isooctane mixture. This seemed unreasonably high so 100% 3-pentanone was tested. The output from the FID was adjusted using the ECN and the error was in the range of 15%. Therefore 3-pentanone and isooctane mixture's response did not follow the method of effective carbon numbers and could only be used for an indicator in this experiment.